International Journal of Scientific Research in Engineering and Management (IJSREM)
Volume: 09 Issue: 11 | Nov - 2025 SJIF Rating: 8.586 ISSN: 2582-3930

ALGAN/GAN HEMT-Based Biosensor for Rapid and Sensitive Detection of Biomolecules

Amulya BV , Priya R

Amruta Institute of Engineering and Management Sciences, Bidadi, Bangalore, India

Guide: Chethana S

Abstract

HEMT technology is being used for development of biosensors. Many floating gate HEMT based biosensors have been experimentally developed but little work has been reported on modeling of MOSHEMT based biosensors. Therefore in this paper an analytical model of AlGaN/GaN MOSHEMT based biosensor has been developed for the first time to detect the biomolecule species such as protein, streptavidin, ChOx, and uricase by using dielectric modulation approach. In this paper cavity length and dielectric constant of MOSHEMT device are optimized to improve the sensitivity of the device. The proposed structure of MOSHEMT has been simulated on ATLAS TCAD device simulator and the simulated results show a significant change in drain current, shift in threshold voltage, change in channel potential below cavity region and capacitance on introducing biomolecules in the nanogap cavity. The results of analytical model have been verified and they show good agreement with simulated results. The sensitivity of the device can be enhanced by optimizing device parameters such as nanogap cavity length, width and also by varying gate length of the device.

Keywords –

Biomolecule, Biosensor, 2DEG (Two Dimentional Electron Gas), MOSHEMT

1. Introduction

The high electron mobility transistor (HEMT) is a heterostructure field effect device.

The most-common heterojunctions for the HEMTs are AlGaN/GaN,AlGaAs/GaAs, AlGaAs/InGaAs and In AlAs/

In GaAs heterointerfaces. Figure 1 shows a schematic view of a conventional AlGaN / GaN HEMT. The main feature of a HEMT is its heterojunction structure. For the HEMT in Figure 1, AlGaN is the wide bandgap semiconductor and GaN is the relatively low bandgap semiconductor. A two-dimensional electron gas(2DEG) layer forms at the hetero interface of AlGaN/GaN high electron mobility transistor(HEMT).

The benefits of high electron mobility transistor (HEMT) based sensors include increased mobility and the formation of two-dimensional electron gas (2DEG), which increases sensitivity and minimizes the risk of static electricity damage[1].

Because of their low cost, repeatable, and predictable electrical response, silicon- based sensors remain the most common, dominating, and readily accessible semiconductor material. The major disadvantage of these sensors is that they are not appropriate for use in harsh conditions such as high temperatures, high pressure, or corrosive environments. Wide bandgap group III nitride compound semiconductors are an alternative to Silicon-based sensors because of their chemical resistance, high temperature or high power capabilities, and high electron saturation velocity[2, 3].

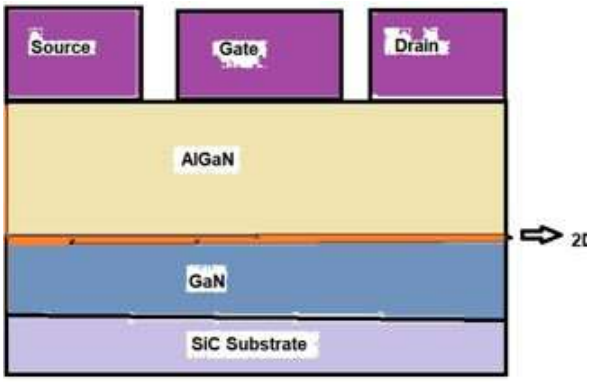

Figure 1 : Conventional schematic structure of AlGaN/GaN HEMT

2. Simulation details

2.1. HEMT device structure

The HEMT device used in this work consists of GaN/Al0.25Ga0.75N/ GaN hetrostructure on a silicon carbide (SiC) substrate. The epilayer structure includes

1.7 µm thick Fe-doped GaN buffer layer, 5 nm undoped GaN channel layer, 22 nm AlGaN barrier layer with 25% Al mole fraction, and 3 nm GaN cap layer. The HEMT features 0.25 µm gate length (*LG*), 200 µm gate width (*WG*), and 50 nm of silicon nitride (SiN) surface passivation. The source-gate (*LSG*) and gate-drain (*LGD*) spacing of the HEMT are 0.8 µm and 2.7 µm, respectively. The schematic cross section of the simulated AlGaN/GaN HEMT structure is illustrated in Fig. 1. The AlGaN/GaN HEMT device structure of Zhang et al. [9] with *LG* = 0.5 µm is also considered for transient simulations. The simulated structure [9] of this HEMT consists of 600 nm GaN buffer layer, 5 nm GaN channel layer, 20 nm Al0.35Ga0.65N barrier layer, 3 nm GaN cap layer, and 50 nm SiN passivation. The device dimensions are *LSG* = 0.5 µm, *LG* = 0.5 µm, *WG* = 100 µm, and *LGD* = 1 µm, respectively.

2.2. Device simulation model

Commercially available Sentaurus TCAD [16] is utilized for the 2D-device simulation studies. The above AlGaN/GaN HEMT structures are created in the simulator. The Schottky work function (WF) is chosen as 4.4 eV for gate contact. The modified

Schottky contact (WF = 4 eV) parameters are used in the source and drain contacts for robustness [16]. Nonlocal electron tunneling is activated with a low tunneling mass of 0.001 mo, so the source and drain contacts are essentially Ohmic. Such contact settings can avoid abrupt band bending near the contact, thereby providing a better convergence in mixed-mode simulations rather than using conventional Ohmic models [16]. To account for the spontaneous and piezoelectric polarization produced charge in the AlGaN/GaN HEMT, fixed charge sheets with equal density (*σpol*) but opposite polarity are placed on the two sides of the AlGaN barrier layer [5–8,10,12,13]. The drift– diffusion model for carrier transport, no bandgap narrowing, temperature dependent mobility model along with high-field saturation dependence, Shockley-Read- Hall (SRH) recombination for trap dynamics modeling, Fermi statistics, and thermionic emission model at heterojunction interface are considered in the physical model. Self-heating effects are not included in the charge transport model, because the HEMTs were fabricated on SiC substrates, which have high thermal conductivity [5,10,12]. Moreover, the self- heating

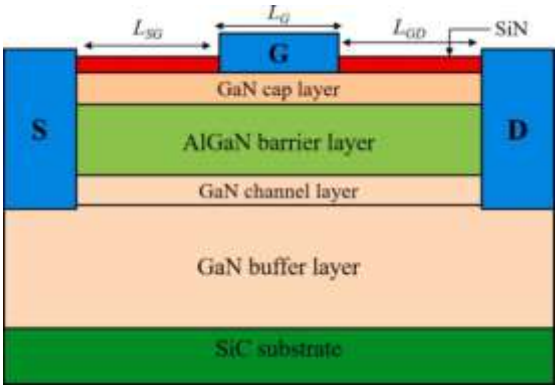

Figure 2 : Schematic cross section of the simulated AlGaN/GaN HEMT structure.

effects in the gate-lag and drain-lag transient characteristics are almost negligible [5,6,10]. From DCTS and LF *Y22* measurements [4], an electron trap at *ETB* = EC □ 0.47 eV (electron capture cross-section *σnB* = ~7 × 10□ 17 cm2) has been identified in the Fe-doped n-type GaN buffer. Accordingly, these values of *ETB* and *σnB*, and hole capture cross-section of *σpB* = 10□ 20 cm2 are used for the acceptor-type buffer trap, to incorporate the effect of compensational Fe-doping in the n-type GaN buffer [12,13,17]. Note that, no traps are considered in the GaN channel layer. Since surface donor energy (*ETS*) is not identified from the DCTS and *Y22* measurements, initially an arbitrary value is chosen for *ETS*. After many iterations, it is found that *ETS* = EC □ 0.5 eV provides a suitable match between the simulated and measured DC, *Y22* and transient characteristics. So, the surface donors are placed at *ETS* = EC □ 0.5 eV at the GaN/ nitride ungated interface [4] and the

electron and hole capture cross sections (σnS and σpS) are taken as 10□ 15 cm2. The surface and buffer trap concentrations are calibrated based on comparison between simulated and measured results. The barrier trap at EC □ 0.45 eV (density of 5 × 1016 cm□ 3) is also included in the model and its influence on the HEMT properties is examined. The LF *Y22* and transient simulations are performed in a mixed-mode circuit environment. Using small signal AC analysis in a two-port network configuration, the imaginary part of the output admittance, *Im {Y22}*, is computed from the RF extraction library [4] and the *Y22* characteristics are acquired in the LF range of 100 Hz to 1 MHz at different temperatures (25–125 ◦C). In DL and GL responses, a transient pulsed source is selected for voltage switching operation at the corresponding gate/drain terminal, while a fixed DC voltage source is considered for other terminal. The resulting drain current (*IDS*) transient response is obtained with respect to time. Note that, the GL transient simulations are prone to the convergence issues, so proper selection of "Math" section in the S-device file is important to attain the GL transients.

3. Structure

Recent studies show that the addition of an ultra-thin AlN spacer layer between AlGaN and GaN, with a thickness of 1 nm (less than the critical thickness of 2DEG), enhances the 2DEG density by removing charge carriers from the barrier AlGaN layer[4, 5]. The presence of an AlN exclusion layer results a significant conduction band offset at the hetero interface which improves the device performance in terms of current, frequency, and power. The structure of developed model of two-dimensional cross sectional AlGaN/AlN/GaN HEMT biosensor for detection of biomolecules has shown in Figure 2 [6].

4. Sensor Model

The output drain current is dependent on the gate bias , according to the charge control model[6]. When biomolecules are immobilized, their impact on device properties will be neutralized by the imposed gate bias. As a result, a floating gate model is necessary to fully assess the effect of channel/2DEG modulation owing to gate immobilization rather than gate

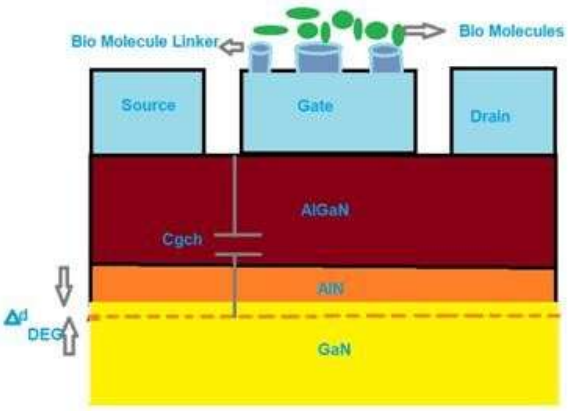

Figure 3:Two-dimensional cross sectional AlGaN/AlN/GaN HEMT biosensor for detection of various *biomolecules*

biasing. The biomolecule poses a certain charge depending on its condition. So due to these charged biomolecules on tha gate a capacitive effect will be felt in the heterojunction layer. As a result more electrons will be accumulated in the 2DEG region for positively charged biomolecules. Similarly electrons will be dissipated for negatively charged biomolecules on the gate due to capacitive effect. Increased electron density in the channel will lead to enhancement of drain current and decreased electron density thereby leading to a decrease in the drain current.

5. Performance of HEMT Based Biosensor in Comparison with Silicon Based Biosensor

Silicon(Si) based biosensor require higher gate charge as well as high bias gate voltage(10-12 V) whereas GaN HEMT biosensors require lower gate charge which decreases driving loss and enables faster switching and to get on state source drain resistance it requires low bias gate voltage(5-6 V). Due to low gate voltage and low output capacitance GaN HEMT are better for high bandwidth applications such as fast switching. Silicon biosensor has a low saturation velocity but GaN HEMT has a high saturation velocity which results in low loss for power devices. GaN HEMT has a capability to operate on a very high temperature but Silicon biosensor can't. In respect of Silicon biosensor, GaN HEMT offers comparatively higher efficiency.

The ID-VG characteristics shown in figure 4 are obtained by introducing the biomolecules in the nanogap cavity region for Wcavity = 20 nm, Lcavity = 500 nm and by operating the device at a drain voltage of 5 V. Figure 4 shows variation of drain current with gate voltage for different biomolecules. The on state current increases with decrease in dielectric constant of biomolecules. The on state current shows good sensitivity as it shows larger change in drain current above subthreshold regime. Figure 4 shows the change in drain current of the device for ChOx, uricase, streptavidin and protein. The dielectric constant of different biomolecules are shown in table I. The ChOx biomolecule shows a small variation of 4.3 mA in drain current but uricase with lesser dielectric constant shows larger change in drain current of 15.9 mA at a gate voltage of -7 V.\

TABLE I
DIELECTRIC CONSTANT OF BIOMOLECULES

Biomolecule	Permittivity
Uricase	1.54
Streptavidin	2.1
Protein	2.50
ChOx	3.30

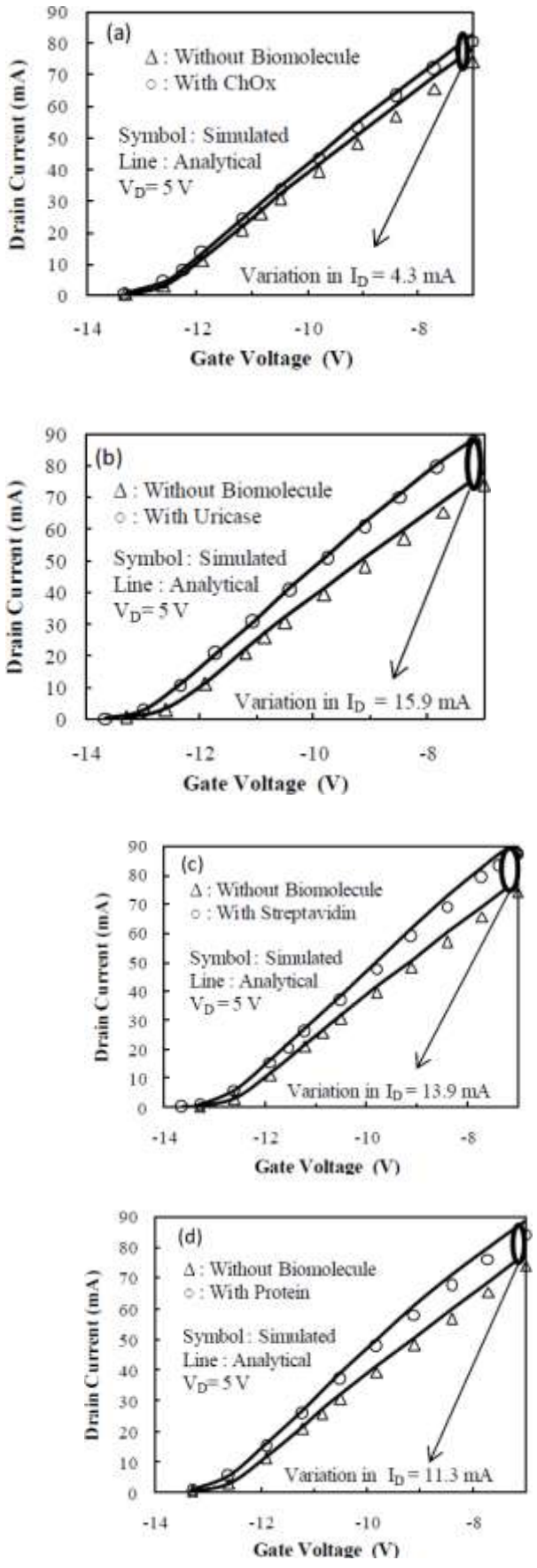

Figure 4: ID-VG for different biomolecules. (a) Variation of drain current for ChOx. (b) Variation of drain current for uricase. (c) Variation of drain current for streptavidin. (d) Variation of drain current for protein.

Simulations have been carried out for drain current of the proposed structure for different drain voltages. Figure 5 depicts that simulated results match well with analytical model. It can be seen that in ID- VD characteristics, highest change in drain current is observed for uricase while for ChOx a least change in drain current is obtained. Drain-on-sensitivity, SIon is defined as: ....(19) In our previous work [36] GAA-JLT has been modeled for subthreshold operation because GAA-JLT shows higher change in off current as compared to on state current but in this work MOSHEMT is modeled for depletion mode operation (above subthreshold) due to higher change in on current because of different conduction mechanism in both the devices. Therefore, sensitivity parameter SIon has been used as figure of merit.

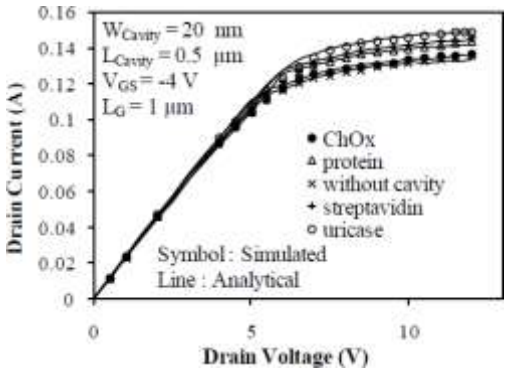

Figure **Error! No text of specified style in document.**5:ID-VD plot of simulated and analytical model for ChOx, protein, streptavidin and uricase biomolecules.

Figure 6 shows the change in SIon parameter for different biomolecules. Among all the biomolecules a maximum change in sensitivity of about 0.0158 is observed for uricase when cavity length is varied from 400 nm to 600 nm. This is because when the cavity length increases, more area is provided for the biomolecules to interact with bio-functionalized layer (AlGaN) which modulates charge density by changing the drain current. The change for uricase is larger because uricase has smaller dielectric constant. Therefore, the results suggest that for high sensitivity applications, the MOSHEMT device should be designed with large cavity length and operated above the subthreshold regime.

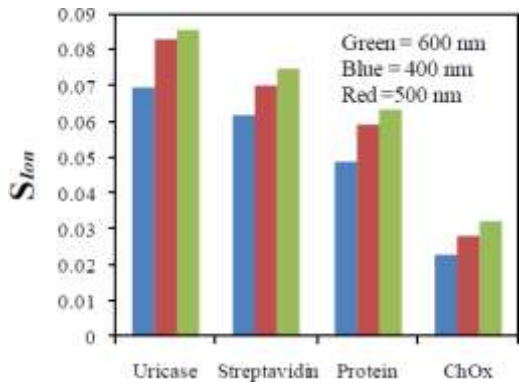

Figure 6: Drain-on sensitivity (SIon) for different biomolecules.

6. Conclusion

AlGaN/GaN, AlGaAs/GaAs based HEMT biosensor has wide range of properties such as increased sensitivity, strong selectivity, specificity, reliability, stability, good repeatability, linearity, chemical and thermal stability, high electron mobility, and reduced device size. These overspread properties ensure the effectiveness of the HEMT device as a biosensor. This groundbreaking biosensor technique has a wide range of applications in biomedical engineering, including pathogen and toxin detection, transplant rejection, troponin I, cell differentiation, early illness diagnosis and prognosis, drug development, medicine, and cellular dynamics research. Detection of cardiovascular disease, protein, DNA, glucose, pH values of solution is possible by this technology. This technique offers a reduction in the cost and time, is simple to integrate into portable systems, and shows promise as a point-of- care diagnostics in the future.

Acknowledgements

The authors thank the faculty and staff of Amruta Institute of Engineering and Management Sciences, Bidadi for their support and guidance.

Reference

[1] K. Mukherjee, F. Darracq, A. Curutchet, N. Malbert, N. Labat, *"TCAD Simulation Capabilities Towards Gate Leakage Current Analysis of Advanced AlGaN/GaN HEMT Devices."*

[2] P. Vigneshwara Raja, J.-C. Nallatamby, N. DasGupta, A. DasGupta, *"Trapping Effects on AlGaN/GaN HEMT Characteristics."*

[3] A. Curutchet, K. Mukherjee, et al., *"Simulation-Based Reliability Assessment of Next-Gen GaN HEMTs under Thermal Stress."*

[4] P. V. Raja, N. DasGupta, et al., *"Gate- Lag and Drain-Lag Simulation in AlGaN/GaN HEMTs Using Mixed-Mode TCAD."*

[5] K. Mukherjee, F. Darracq, *"Optimization of Gate Tunneling Parameters in GaN HEMTs for Leakage Reduction."*

[6] Praveen Pal, Yogesh Pratap, Mridula Gupta, Sneha Kabra, *"Modeling and Simulation of AlGaN/GaN MOS-HEMT for Biosensor Applications."*

[7] Chenbi Li, Xinghuan Chen, Zeheng Wang, *"Review of the AlGaN/GaN High- Electron-Mobility Transistor-Based Biosensors: Structure, Mechanisms, and Applications."*

[8] Hee Ho Lee, Myunghan Bae, Jang- Kyoo Shin et al., *"AlGaN/GaN High Electron Mobility Transistor-Based Biosensor for the Detection of C-Reactive Protein."*

[9] Mishra, Chaturvedi, and colleagues, *"Simulation and Experimental Study of HER2 Detection Using AlGaN/GaN HEMT-Based Biosensor."*

[10] Chen et al., Wang et al., *"Design and Optimization of GaN HEMT Biosensors for Cancer Biomarker Detection."*

[11] Hiu Y. Wong, Nelson Braga, R.V. Mickevicius, Feng Gao, Tomás Palacios, *"Study of AlGaN/GaN HEMT Degradation through TCAD Simulations."*

[12] Stephan Strauss, Axel Erlebach, Tommaso Cilento, Denis Marcon, Steve Stoffels, Benoit Bakeroot, *"TCAD Methodology for Simulation of GaN-HEMT Power Devices."*

[13] Praveen Pal, Yogesh Pratap, Mridula Gupta, Sneha Kabra, *"Modeling and Simulation of AlGaN/GaN MOS-HEMT for Biosensor Applications."*

[14] F. Gao, T. Palacios, et al., *"Advanced GaN-Based HEMT Simulation for Reliability and Power Applications."*

[15] P. Pal, S. Kabra, Y. Pratap, *"Enhanced Analytical Modeling of AlGaN/GaN MOSHEMTs for Biomedical Sensing."*